

# A LIGHTWEIGHT FEATURE FUSION ARCHITECTURE FOR RESOURCE-CONSTRAINED CROWD COUNTING

Yashwardhan Chaudhuri<sup>1\*</sup>, Ankit Kumar<sup>2\*</sup>, Orchid Chetia Phukan<sup>1</sup>, Arun Balaji Buduru<sup>1</sup>

<sup>1</sup>IIT Delhi, India

<sup>2</sup>IIT Bombay, India

## ABSTRACT

Crowd counting finds direct applications in real-world situations, making computational efficiency and performance crucial. However, most of the previous methods rely on a heavy backbone and a complex downstream architecture that restricts the deployment. To address this challenge and enhance the versatility of crowd-counting models, we introduce two lightweight models. These models maintain the same downstream architecture while incorporating two distinct backbones: MobileNet and MobileViT. We leverage Adjacent Feature Fusion to extract diverse scale features from a Pre-Trained Model (PTM) and subsequently combine these features seamlessly. This approach empowers our models to achieve improved performance while maintaining a compact and efficient design. With the comparison of our proposed models with previously available state-of-the-art (SOTA) methods on ShanghaiTech-A ShanghaiTech-B and UCF-CC-50 dataset, it achieves comparable results while being the most computationally efficient model. Finally, we present a comparative study, an extensive ablation study, along with pruning to show the effectiveness of our models.

## 1. INTRODUCTION

Crowd counting refers to the estimation of the number of people in a crowd scene from either an image or a video, which found numerous applications that hold significant societal relevance, including urban planning, area footfall estimation, and crowd management. Crowd counting is a challenging problem because of the diverse behavior of crowds, heavy occlusions, and complex backgrounds. Recently, CNN-based networks have made remarkable progress, having a heavy architecture that demands substantial resources and computation costs, which restricts their deployment scopes and causes poor scalability. Many methods focus on dealing with this problem propose lightweight architectures, utilize pruning [1] [2] and Quantization[3] [4], Although effective, these following methods suffer from meticulous hyperparameter tuning and hardware limitations. Moreover, the following methods

can also significantly affect model generalization due to a regularization effect. Other methods [5] [6] utilize knowledge distillation-based method that makes use of supervision from a large model (teacher) to train a smaller model (student). While this technique enhances the performance of the student model, it also requires additional training time and careful selection of teacher models for better learning. These methods push heavy models to become lightweight, but the inherent computational resource requirement and model size remain massive from the perspective of existing lightweight works. To address these challenges, We propose Adjoining Semantics Fusion Network (ASFNet), a lightweight crowd-counting network generating density maps by progressively fusing adjacent feature sets at each level, as shown in figure 1. ASFNet comes in two variations: ASFNet-B and ASFNet-S. Both of these architectures share a common downstream network but are characterized by their distinct backbones. It involves a small number of parameters and achieves satisfying performance on benchmark datasets. The key contributions are as follows:

- We propose ASFNet-S and ASFNet-B, two varieties of lightweight architectures with different backbones and common downstream networks for resource-efficient crowd-counting. We utilize the adjacent feature fusion technique, which merges different scale features for easier feature integration and improved learnability.
- Evaluation of our models on benchmark datasets such as ShanghaiTech-A, ShanghaiTech-B and UCF-CC-50, shows comparable performance with SOTA works across various metrics with significantly less parameters, FLOPs and inference time.
- Ablation study to find the efficacy of our model; through extensive experiments, ablation study, and pruning analysis, we confirm the viability of our model architecture.

## 2. RELATED WORK

Most recent crowd-counting methods employ CNN to predict density maps from crowd images. MCNN [7] employs a multi-column architecture that effectively captures scale

\*Authors contributed equally as first authors

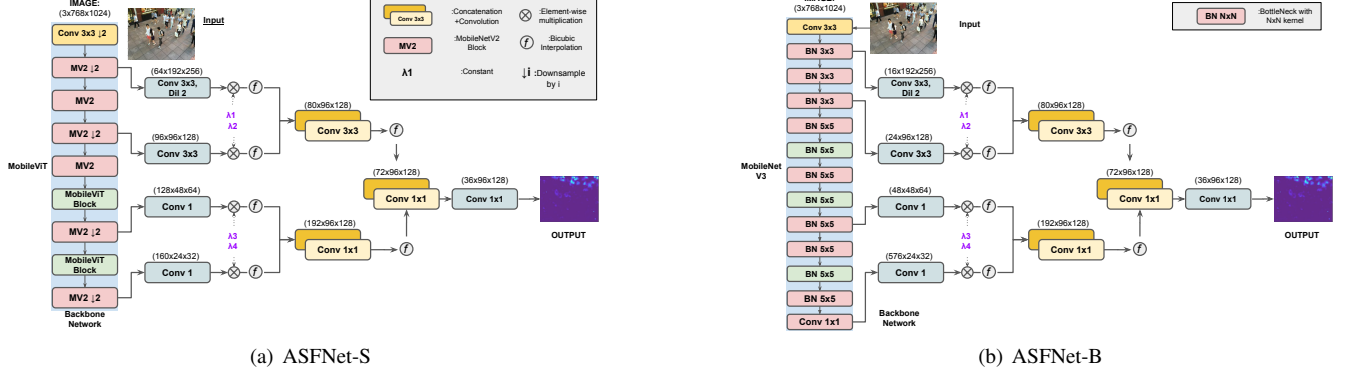


**Fig. 1:** The overall architectural depiction of ASFNet-B and ASFNet-S illustrates ASFNet-S leverages a MobileViT backbone, while ASFNet-B employs a MobileNet backbone, common downstream shared by both networks, enabling multi-scale feature extraction.

variation. CSRNet [8] CANNET[9] use single-column with dilated convolution layer. In [10], the convolution filter is replaced by locally connected Gaussian kernels called GauNet and proposes a low-rank approximation for the translation invariance problem. MSSRM[11] propose a Multi-Scale Super-Resolution Module that guides the network to estimate the lost details and enhances the detailed information. These methods perform well, but they are large in size and computationally expensive. Some lightweight architecture [12] [13] [14] use feature fusion and quantization, which are hardware-dependent architecture.[5] purpose Structured Knowledge Transfer (SKT) framework that maximizes the utilization of structured knowledge from a proficiently but depends on a trained teacher network to produce a streamlined student network.Lw Count[15] SANet[16] propose an encoding-decoding-based lightweight crowd-counting network. Furthermore, in our work, we explore,

### 3. METHODOLOGY

#### 3.1. Proposed Architecture

We propose two different architectures, ASFNet-S and ASFNet-B, as shown in Figure 1, having the same downstream network with different backbones, i.e. MobileViT<sup>1</sup>[17] for ASFNet-B and MobileNetV3<sup>2</sup>[18] for ASFNet-S. Each has two key components: a pre-trained backbone for feature extraction and a downstream network with adjacent feature fusion responsible for density map generation. The pretrained backbone is typically a deep neural network previously trained on a large dataset imagenet, serving to extract multiscale features from input data. The downstream network follows the backbone and further processes these features, with adjacent feature fusion indicating that feature fusion happens in a nearby and sequential manner within the network. This fusion combines features from different levels

of abstraction, allowing the network to benefit from low-level and high-level information for density map generation.

#### 3.2. Feature Extraction

MobileNet and MobileVit are well-suited backbone networks for lightweight crowd-counting tasks primarily because of their efficiency and speed, making them an excellent choice for resource-constrained and real-time applications. MobileNetV3 is an efficient convolutional neural network designed for fast deep learning on mobile devices. It achieves efficiency through depthwise separable convolutions and maintains accuracy with inverted residual blocks. The MobileViT block combines standard convolutions and transformers to capture local and global representations. It Replaces local processing with a stack of transformer layers gains convolution-like properties while learning global context efficiently. We utilize the four blocks of the backbone network to capture diverse feature information at different levels of semantic information, with initial layers having low-level semantic information and the later layers having high-level semantic information. The output of the feature extraction block is passed sequentially to the downstream network, which uses the adjacent feature fusion technique for density map generation.

#### 3.3. Adjacent Featutres

Given an input image  $I_i \in \mathbb{R}^{C_i \times H_i \times W_i}$ , where  $C_i$  refers to the number of channels,  $H_i$  is Height, and  $W_i$  is the width of the image,  $I_i$  is fed into the backbone network to obtain four different sets of multi-scale feature maps  $\{F_1, F_2, F_3, F_4\}$  from intermediate layers as shown in Figure 2. Using larger kernel sizes in CNN increases the number of parameters and FLOPs. This happens because larger kernels have more weights to learn, resulting in a higher parameter count, and they require more computations during forward and backward passes, leading to increased FLOPs. Therefore, it's important

<sup>1</sup><https://huggingface.co/apple/mobilevit-small>

<sup>2</sup>[https://download.pytorch.org/models/mobilenet\\_v3\\_small-047dcff4.pth](https://download.pytorch.org/models/mobilenet_v3_small-047dcff4.pth)

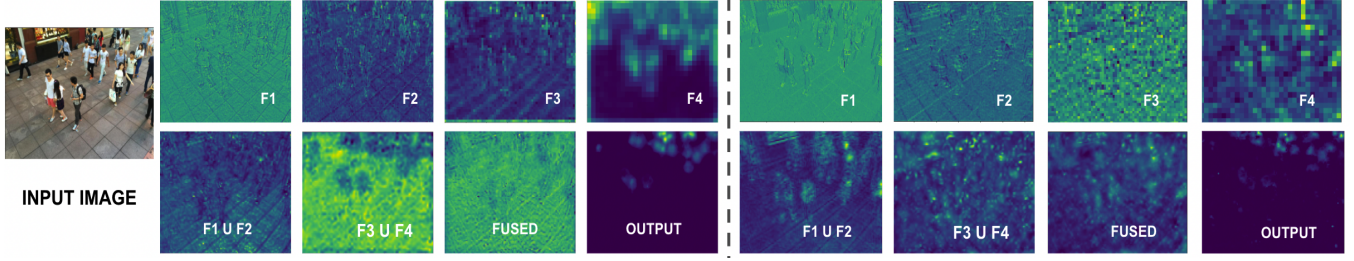


**Fig. 2:** Left: Feature maps from each layer of ASFNet-B, Right: Feature maps from each layer of ASFNet-S. Where F1, F2, F3 and F4 shows the different scale features and features from intermediate layers.

to strike a balance between kernel size and computational efficiency when designing CNN architectures to avoid unnecessary complexity and resource usage, so we set  $\{(3 \times 3, \text{dil} = 2), (3 \times 3), (1 \times 1), (1 \times 1)\}$  as kernels for the given four sets of feature maps. After applying the convolution operation  $\mathcal{H}_i$  followed by ReLU activation  $\gamma$ , we multiply each feature  $F^i$  by a parameter  $\lambda_i$ , which reduces the noise in the feature map.

$$F'_i = \lambda_i(\gamma(\mathcal{H}_i(F_i))) \quad (1)$$

where  $i, k=1,2,3,4$ . We then apply bicubic interpolation for every feature map to rescale every feature map to a similar dimension. The interpolated pixel value at coordinates  $(x, y)$  can be expressed using bicubic interpolation as follows:

$$\mathcal{F}_{inter}(x, y) = \sum_{i=0}^3 \sum_{j=0}^3 w_{ij} \cdot F_k(x+i, y+j) \quad (2)$$

Where  $F_k(x+i, y+j)$  represents the pixel values of the neighbouring pixels within the local  $4 \times 4$  neighbourhood around  $(x, y)$  and  $w_{ij}$  are the bicubic interpolation weights. Then we concatenate adjacent scaled features map  $F'_1, F'_2$  and  $F'_3, F'_4$  to get  $\{f_{fuse}^1, f_{fuse}^2\}$  as a set of new feature maps; We do this to process similar complexity of semantics at each level. The process continues till we reach the final set of feature maps  $f_{net}$  that goes through  $1 \times 1$  convolutions to generate the final density map. The mathematics is as described below.

$$f_{fuse}^i(a, b) = \gamma(\mathcal{H}_i(F'_a \cup F'_b)) \quad (3)$$

$$F_{fused} = \gamma(\mathcal{H}_{fused}(\bigcup_{i=1}^2 f_{fuse}^i(2i, 2i-1))) \quad (4)$$

$$f_{net} = \gamma(\mathcal{H}_{net}(F_{fused})) \quad (5)$$

### 3.4. Loss Function

Our final output is a 2-dimensional density map; hence, we use a pixel-wise L2 loss function that compares each pixel value in the density map corresponding to its ground truth.

$$L(\Theta) = \frac{1}{2n} \sum_{i=1}^n \|h(\theta, x_i) - G\|_2^2 \quad (6)$$

Where  $n$  is the size of the training set, and  $x_i$  represents the  $i_{th}$  input image.  $h(\Theta, x_i)$  is the output and  $G$  is ground truth density map of image.  $L(\Theta)$  denotes the loss between the ground-truth density map and the estimated density map.

## 4. EXPERIMENTS

**Dataset:** Our experiments are conducted on three benchmark datasets: ShanghaiTech (Part A and Part B) and the UCF-CC-50 dataset. In ShanghaiTech Part A, a total of 482 crowd images were divided into 300 training images and 182 testing images. The average number of pedestrians in these images was approximately 501. Meanwhile, ShanghaiTech Part B contained 716 images, with 400 allocated for training and 316 for testing. In contrast to Part A, the average pedestrian count in Part B was notably smaller, averaging around 123 pedestrians per image. The UCF CC 50 dataset consisted of 50 images with high crowd density, featuring varying pedestrian counts, ranging from 94 to 4,543 pedestrians per image.

**Ground Truth Generation:-** We follow [7] To generate a ground truth density map that uses the geometry-adaptive kernels; due to invariance in the crowd, we generate the ground truth density maps with the spatial distribution information across the whole image. The geometric adaptive Gaussian kernel is given as

$$F(x) = \sum_{i=1}^N \delta(x - x_i) * G_{\sigma_i}, \quad \sigma_i = \beta \bar{d}_i \quad (7)$$

where  $\sigma_i = \beta \bar{d}_i$ ,  $x_i$  represents a specific target object within the ground truth  $\delta$ . To transform  $\delta(x - x_i)$  into a density map, we convolve it with a Gaussian kernel having a standard deviation of  $\sigma_i$ . Here,  $\bar{d}_i$  signifies the average distance among the  $k$  nearest neighbours of the target object  $x_i$ ; for our experiment, we set  $k = 10$ .

**Evaluation metrics:-** Followed by the previous crowd counting model [7] [9], we use Mean Squared Error (MSE) and Mean absolute error (MAE) standard measures for evaluating the effectiveness and accuracy of our model. To assess the lightweightness, number of parameters, Floating Point Operation (FLOP) and model size are considered as well-suited metrics.

Methods	ShanghaiTech A		ShanghaiTech B		UCF-CC-50		#Param	FLOPs	Size(MB)	Inference(s)
	MSE	MAE	MSE	MAE	MSE	MAE				
CSRNet[8]	115.0	68.2	16.0	10.6	397.5	266.1	16.26	649.813	62.05	36.56
CANNet[9]	100	62.3	12.2	7.8	243.7	212.2	18.12	688.526	69.09	90.34
ASPDNet[19]	96.2	60.8	10.5	7.2	-	-	27.42	911.108	104.63	255
SCARNet[20]	144.1	66.3	15.2	9.5	-	-	16.28	650.388	62.16	84.98
P2PNet[21]	85.1	52.7	9.9	6.3	256.1	172.7	18.34	-	82.3	-
UEPNet[22]	91.2	54.6	10.9	6.4	131.7	81.1	26.21	-	-	-
SANet[16]	122.2	75.3	17.9	10.5	334.9	258.4	0.91	-	-	-
MCNN[7]	173.2	110.2	41.3	26.4	509.1	377.6	0.133	42.26	0.53	5.38
TDFCNN[23]	145.1	97.5	32.8	20.7	491.4	354.7	0.13	-	-	-
C-CNN[12]	141.7	88.1	22.1	14.9	-	-	0.073	19.830	0.23	0.8
ACSCP[24]	102.7	75.7	27.4	17.2	404.6	291.0	5.10	-	-	-
ASFNet-S	91.67	61.09	18	11.2	252.3	192.1	2.58	2.185	15.5	27
ASFNet-B	88.67	59.32	11.02	8.2	151.49	106.69	5.69	29.803	10.6	71.2

**Table 1:** Comparison with state-of-the-art methods. #Param denotes the number of parameters, while FLOPs is the number of Floating Point Operations, and Size is the size of the trained model. Execution time is computed on an Nvidia T400 GPU. The units are million (M) for #Param, giga (G) for FLOPs, millisecond (ms) for GPU time, and size is in MegaByte (MB). The entire table is divided into two parts: the upper one contains heavy models, while the lower part contains lightweight models. Blue colour shows the SOTA result, and red shows the best performance among lightweight models.

**Training Details:** We train both models using the same hyperparameters and as the Adam optimizer with a learning rate of  $5e-5$  and weight decay as  $1e-4$ . After experimenting with various combinations, our experiments have empirically shown that appropriate values of  $\lambda_1=0.1$ ,  $\lambda_2=0.1$ ,  $\lambda_3=0.5$ ,  $\lambda_4=1.0$ . We train both models on Tesla T4 GPU for 500 epochs.

## 5. RESULTS

We evaluate our proposed lightweight models with previous state-of-the-art (SOTA) work on three datasets, as shown in Table 1, considering key metrics such as MSE, MAE, inference time, number of parameters, and model size. Our findings show that the proposed models acquire a balance between performance and efficiency. ASFNet-B achieves comparable results to the SOTA across all three datasets while utilizing fewer parameters, requiring lower FLOPs, exhibiting a smaller model size, and demonstrating faster inference times. Meanwhile, ASFNet-S excels in the lightweight category, particularly in terms of MSE, MAE, and FLOPs, however, with a slight increase in parameters and model size. To the best of our knowledge, we have the lowest FLOPs in comparison to existing works.

## 6. ABLATION STUDY

To evaluate the effectiveness of our approaches, we conducted a series of experiments for ablation study, as shown in Table 2, where we fused different feature groups instead of adjacent features and found that fusing adjacent features gives the best results. We conducted experiments to assess the impact of weighted convolutions by comparing the model’s accuracy when trained with and without the use of weight and it has

been observed a slight decrease in the model’s performance when we excluded the convolutional weights from the training process. Additionally, we examined the effects of 25% L1 and 25% L2 pruning techniques on the model’s performance as shown in Table 3

**Table 2:** Ablation Study of ASFNet-B on ShanghaiTech-B Benchmark Dataset with different feature set fusions and non-weighted convolutions.

Combination(ASFNet-B)	ShanghaiTech-B	
	MSE	MAE
fuse(F1, F3), fuse(F2, F4)	14.07	8.61
fuse(F1, F4), fuse(F2, F3)	13.32	8.48
fuse(F1, F2), fuse(F3, F4)	11.02	8.2
No weights	13.75	8.12

**Table 3:** L1 Pruning and L2 Pruning on ASF-Net-B. Evaluated on ShanghaiTech-B Dataset

DATASET	L1 Pruning		L2 Pruning	
	MSE	MAE	MAE	MSE
ShanghaiTech A	118.1	73.2	160.1	92.8
ShanghaiTech B	32.25	17.52	34.57	19.60
UCF-CC-50	390	270.2	440.7	312.21

## 7. CONCLUSION

In this work, we propose a simple yet computationally efficient model called ASFNet, giving comparable accuracy to multiple SOTA models at substantially lesser parameter count, FLOPs count, and model size. We support our claims with extensive experiments. Although The models prove efficient, the ASFNet-B model has a slightly larger inference time than its competitors. Reducing inference time in ViT-based crowd regression architectures can be a future research

direction.

## 8. REFERENCES

- [1] Sajid Anwar, Kyuhyeon Hwang, and Wonyong Sung, “Structured pruning of deep convolutional neural networks,” *ACM Journal on Emerging Technologies in Computing Systems (JETC)*, vol. 13, no. 3, pp. 1–18, 2017.
- [2] Hanyu Peng, Jiaxiang Wu, Shifeng Chen, and Junzhou Huang, “Collaborative channel pruning for deep networks,” in *International Conference on Machine Learning*. PMLR, 2019, pp. 5113–5122.
- [3] Darryl Lin, Sachin Talathi, and Sreekanth Annapureddy, “Fixed point quantization of deep convolutional networks,” in *International conference on machine learning*. PMLR, 2016, pp. 2849–2858.
- [4] Jiwei Yang, Xu Shen, Jun Xing, Xinmei Tian, Houqiang Li, Bing Deng, Jianqiang Huang, and Xian-sheng Hua, “Quantization networks,” in *Proceedings of the IEEE/CVF Conference on Computer Vision and Pattern Recognition*, 2019, pp. 7308–7316.
- [5] Lingbo Liu, Jiaqi Chen, Hefeng Wu, Tianshui Chen, Guanbin Li, and Liang Lin, “Efficient crowd counting via structured knowledge transfer,” in *Proceedings of the 28th ACM international conference on multimedia*, 2020, pp. 2645–2654.
- [6] Benlin Liu, Yongming Rao, Jiwen Lu, Jie Zhou, and Cho-Jui Hsieh, “Metadistiller: Network self-boosting via meta-learned top-down distillation,” in *Computer Vision—ECCV 2020: 16th European Conference, Glasgow, UK, August 23–28, 2020, Proceedings, Part XIV 16*. Springer, 2020, pp. 694–709.
- [7] Yingying Zhang, Desen Zhou, Siqin Chen, Shenghua Gao, and Yi Ma, “Single-image crowd counting via multi-column convolutional neural network,” in *Proceedings of the IEEE conference on computer vision and pattern recognition*, 2016, pp. 589–597.
- [8] Yuhong Li, Xiaofan Zhang, and Deming Chen, “Csrnet: Dilated convolutional neural networks for understanding the highly congested scenes,” in *Proceedings of the IEEE conference on computer vision and pattern recognition*, 2018, pp. 1091–1100.
- [9] Weizhe Liu, Mathieu Salzmann, and Pascal Fua, “Context-aware crowd counting,” in *Proceedings of the IEEE/CVF conference on computer vision and pattern recognition*, 2019, pp. 5099–5108.
- [10] Zhi-Qi Cheng, Qi Dai, Hong Li, Jingkuan Song, Xiao Wu, and Alexander G Hauptmann, “Rethinking spatial invariance of convolutional networks for object counting,” in *Proceedings of the IEEE/CVF Conference on Computer Vision and Pattern Recognition*, 2022, pp. 19638–19648.
- [11] Jiahao Xie, Wei Xu, Dingkan Liang, Zhanyu Ma, Kongming Liang, Weidong Liu, Rui Wang, and Ling Jin, “Super-resolution information enhancement for crowd counting,” in *ICASSP 2023-2023 IEEE International Conference on Acoustics, Speech and Signal Processing (ICASSP)*. IEEE, 2023, pp. 1–5.
- [12] Xiaowen Shi, Xin Li, Caili Wu, Shuchen Kong, Jing Yang, and Liang He, “A real-time deep network for crowd counting,” in *ICASSP 2020-2020 IEEE International Conference on Acoustics, Speech and Signal Processing (ICASSP)*. IEEE, 2020, pp. 2328–2332.
- [13] Yabin Wang, Zhiheng Ma, Xing Wei, Shuai Zheng, Yaowei Wang, and Xiaopeng Hong, “Eccnas: Efficient crowd counting neural architecture search,” *ACM Transactions on Multimedia Computing, Communications, and Applications (TOMM)*, vol. 18, no. 1s, pp. 1–19, 2022.
- [14] Kyujin Shim, Junyoung Byun, and Changick Kim, “Multi-step quantization of a multi-scale network for crowd counting,” in *2020 IEEE International Conference on Image Processing (ICIP)*, 2020, pp. 683–687.
- [15] Yanbo Liu, Guo Cao, Hao Shi, and Yingxiang Hu, “Lw-count: An effective lightweight encoding-decoding crowd counting network,” *IEEE Transactions on Circuits and Systems for Video Technology*, vol. 32, no. 10, pp. 6821–6834, 2022.
- [16] Xinkun Cao, Zhipeng Wang, Yanyun Zhao, and Fei Su, “Scale aggregation network for accurate and efficient crowd counting,” in *Proceedings of the European conference on computer vision (ECCV)*, 2018, pp. 734–750.
- [17] Shakti N Wadekar and Abhishek Chaurasia, “Mobilevitv3: Mobile-friendly vision transformer with simple and effective fusion of local, global and input features,” *arXiv preprint arXiv:2209.15159*, 2022.
- [18] Andrew G Howard, Menglong Zhu, Bo Chen, Dmitry Kalenichenko, Weijun Wang, Tobias Weyand, Marco Andreetto, and Hartwig Adam, “Mobilenets: Efficient convolutional neural networks for mobile vision applications,” *arXiv preprint arXiv:1704.04861*, 2017.
- [19] Guangshuai Gao, Qingjie Liu, and Yunhong Wang, “Counting from sky: A large-scale data set for remote sensing object counting and a benchmark method,” *IEEE Transactions on Geoscience and Remote Sensing*, vol. 59, no. 5, pp. 3642–3655, 2020.
- [20] Junyu Gao, Qi Wang, and Yuan Yuan, “Scar: Spatial/channel-wise attention regression networks for crowd counting,” *Neurocomputing*, vol. 363, pp. 1–8, 2019.
- [21] Qingyu Song, Changan Wang, Zhengkai Jiang, Yabiao Wang, Ying Tai, Chengjie Wang, Jilin Li, Feiyue Huang, and Yang Wu, “Rethinking counting and localization in crowds: A purely point-based framework,” in *Proceedings of the IEEE/CVF International Conference on Computer Vision*, 2021, pp. 3365–3374.
- [22] Changan Wang, Qingyu Song, Boshen Zhang, Yabiao Wang, Ying Tai, Xuyi Hu, Chengjie Wang, Jilin Li, Jiayi Ma, and Yang Wu, “Uniformity in heterogeneity: Diving deep into count interval partition for crowd counting,” in *Proceedings of the IEEE/CVF International Conference on Computer Vision*, 2021, pp. 3234–3242.
- [23] Deepak Babu Sam and R Venkatesh Babu, “Top-down feedback for crowd counting convolutional neural network,” in *Proceedings of the AAAI conference on artificial intelligence*, 2018, vol. 32.
- [24] Zan Shen, Yi Xu, Bingbing Ni, Minsi Wang, Jianguo Hu, and Xiaokang Yang, “Crowd counting via adversarial cross-scale consistency pursuit,” in *Proceedings of the IEEE Conference on Computer Vision and Pattern Recognition (CVPR)*, June 2018.